

# A LINEAR BEAM RASTER SYSTEM FOR THE EUROPEAN SPALLATION SOURCE?

H.D. Thomsen\*, A.I.S. Holm, S.P. Møller, ISA, Aarhus University, 8000 Aarhus C, Denmark

## Abstract

The European Spallation Source (ESS) will, when built, be the most intense neutron source in the world. The neutrons are generated by a high power (5 MW) proton beam impacting a rotating W spallation target. To reduce the replacement frequency of components subjected to the full beam current, *i.e.* the proton beam window (PBW) and the target, means to introduce low peak current densities, *i.e.* flat transverse beam profiles, are necessary. The ESS will nominally operate with an average (peak) proton current of 2.5 mA (62.5 mA) at 2.0 GeV. The relatively long beam pulse duration of 2.86 ms (at 14 Hz) leaves ample time to facilitate a Lissajous-like, linear raster system that illuminates a footprint area by sweeping an only moderately enlarged linac beamlet. The design, specifications, performance, and benefits of the beam raster system will be described and discussed.

## INTRODUCTION

At the end of the High Energy Beam Transport (HEBT) [1], the linac beam, having a small normalized transverse rms emittance ( $\varepsilon_w \simeq 0.3 \pi \times \text{mm} \times \text{mrad}$ ,  $w = x, y$ ), needs to transversely match a macroscopic area of  $160 \text{ mm} \times 60 \text{ mm}$  ( $H \times V$ ), the target surface nominal footprint (NFP). Employing a non-linear DC magnet system to generate relatively flat transverse beam profiles has been considered for a long time for the ESS [1]. The non-linear magnets impose a number of constraints on the beam optics to ensure cancellation of higher-order focusing terms and avoid coupling of the transverse planes.

Through a number of linac design iterations, the non-linear system has been tested with several different multi-particle distributions resulting from linac + HEBT end-to-end simulations. As the linac beam pulse is expanded to macroscopic dimensions, the effect of unintentional non-linear aberrations and the characteristics of the transverse halo can be excessively amplified and lead to beam losses. The studies have revealed that the non-linear systems are not particularly robust towards the slight changes in the test input distribution, and relative beam losses of the order of  $10^{-5}$  are prematurely introduced in the final drift region upstream of the target. In particular, the beam losses are very sensitive to the beam transverse kurtosis, *i.e.* the halo extent and magnitude. With a beam power of 5 MW, primary beam losses need, however, to be controlled to an

unprecedented relative level to avoid component activation and neutron backgrounds.

As an alternative, the idea of implementing a fast 2D raster magnet (RM) system is currently being explored. Such a system would need to facilitate *a)* magnification of the linac beam size, and *b)* oscillating deflections acting in both transverse planes. Both goals can be achieved using only linear elements, *i.e.* quadrupoles and dipole RMs, thus avoiding the here unjustified complexity of understanding and tuning non-linear optics.

Since the beam is only slightly magnified to a “beamlet” typically much smaller than the raster pattern amplitudes, excessive magnification of the transverse beam halo is also avoided. This will effectively be smeared out through the pattern and only affects the edge of the accumulated distribution, corresponding to a fraction of the delivered beam. Due to the finite pattern cycle time, the RM concept is only suitable for long-pulse or CW machines. Implementation of beam raster systems has been considered also in other high-power proton machines, typically at raster frequencies of 10–100’s of Hz [2, 3, 4] but also at 10’s of kHz [5]. To minimize raster-induced neutron intensity oscillations at the highly specialized neutron instruments, only the latter frequency range is applicable to the ESS.

## RASTER PATTERN

For the beamlet to map out the rectangular NFP and achieve good uniformity, a linear Lissajous pattern is exploited. The raster pattern is here dictated by the ratio of the sweep frequencies,  $f_y/f_x$ , and the waveform shape and relative phase. The raster pattern cycle time should ideally be a multiple of the nominal macropulse duration,  $\Delta t_p = 2.86 \text{ ms}$ ,  $f_w = n_w/\Delta t_p$ , thus ensuring a closed pattern. If the integers are chosen as appropriate prime numbers, the rational feature of the ratio is minimized, thus avoiding beat patterns. Excessive turning times near the raster waveform amplitudes  $a_w$  can introduce intensity ridges that are particularly pronounced when the relative beamlet size  $\text{rms}(w)/a_w$  is small. Choosing triangular-like waveforms minimizes the risk of such burn-ins and increases the uniformity of the accumulated distribution.

In Table 1, example parameters are displayed, and the resulting pattern is represented by  $5 \times 10^4$  sampled centroid positions, shown in Fig. 1, left panel. Clearly, the beamlet size is modest relative to the amplitudes but large relative to the mesh density, thus leading to a very uniform intensity distribution in the central region. A beamlet distribution has been prepared by tracking  $10^6$  multi-

\* heinetho@phys.au.dk

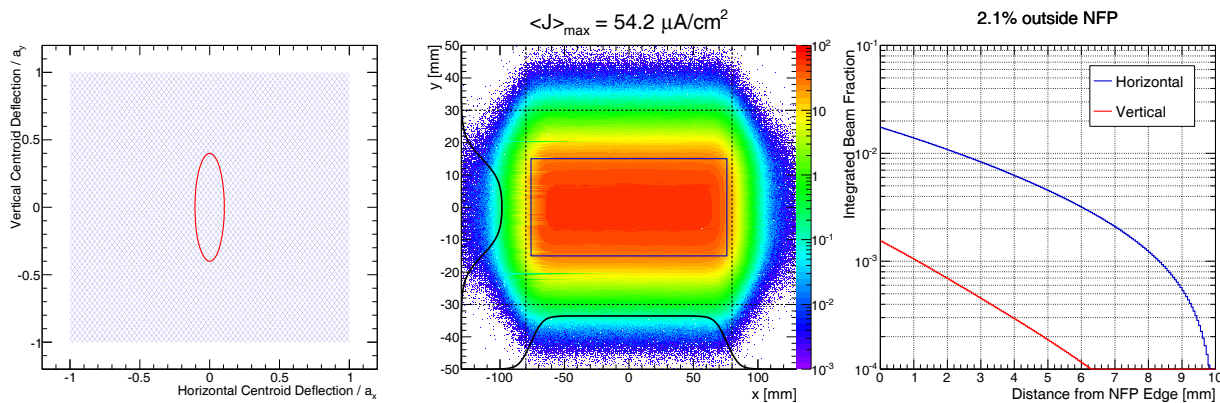


Figure 1: The beam delivered to the target. *Left panel*: a Lissajous-like pattern illustrated by  $5 \times 10^4$  sampled centroid positions generated from the parameters in Table 1. The relative 1-rms beamlet size ellipse is shown with red. *Middle panel*: simulation of the accumulated distribution after having rastered an ESS beamlet for  $\Delta t_p$ . The NFP is marked by dashed lines and the raster pattern outline is displayed by a blue rectangle. *Right panel*: The relative beam deposited outside the NFP.

Table 1: Possible Pattern and Beamlet Parameters

Parameter	Unit	$w = x$	$w = y$
$n_w$	—	83	113
$f_w$	kHz	29.05	39.55
$a_w$	mm	76	15
$\text{rms}(w)$	mm	8.0	6.0

particles of the baseline linac output through the HEBT. At each of the  $5 \times 10^4$  beamlet centroid coordinates,  $2 \times 10^4$  multi-particles are randomly chosen from the  $10^6$  ensemble and projected on a histogram. The resulting distribution is scaled to represent the time-averaged current density  $\langle J \rangle$  normalized to 2.5 mA current, cf. Fig. 1, middle panel. The distribution does not contain any strong intensity structures or artefacts generated by the expander system. Especially the horizontal profile has a wide uniform plateau bound by smooth edges.

Only few % of the beam will be allowed outside the NFP, and the restrictions are particularly strong in the vertical plane due to the limited target wheel height. The right panel of Fig. 1 shows the integrated beam fraction at a distance beyond the NFP border. In the simulated example, only 2.1% of the beam lies outside the NFP, and there is an order of magnitude between the content in the horizontal and vertical plane.

## BEAM OPTICS

The RM beam expander optics is modelled at  $E = 2.5$  GeV, the maximum beam energy currently expected in a machine upgrade scenario, *i.e.* 19% above the nominal rigidity. After a vertical achromatic elevation upstream, the beam is at target level,  $y = 4500$  mm above the linac [1]. The optics is shown in Fig. 2 and the primary magnetic elements comprise 6 DC quadrupoles and  $n_{\text{RM}} = 8$  RMs, 4

acting in each plane. The latter are expected to be mechanically identical—300 mm long with  $80 \times 80$  mm<sup>2</sup> ID vacuum aperture—and placed with mirror-symmetry around the action point (AP), the apparent origin of the deflection in both planes. The downstream quadrupole doublet not only ensures the final beam size expansion, but their strengths are fixed to set a transverse phase advance of  $\pi$  between the AP and the beam crossover (CO), where the centroid displacement introduced by the RMs is hence neutralized by design. To balance the necessary RM peak fields, *i.e.* compensate for the  $\simeq 5:1$  aspect ratio of the pattern amplitudes, the CO doublet provides a horizontal to vertical angular magnification of 6.4:1. At  $f_x, f_y \simeq$  kHz, the feasibility of the dithering RMs is believed to greatly increase by a reduction in peak field. This transport line concept is highly inspired by the MTS line [5]. As the AP→CO phase advance dictates the CO quadrupole strengths, the upstream  $2 \times$  doublet matching section provides the full means to adjust the transverse beamlet size at the CO and target. Scattering in the PBW can also be partially compensated by adjusting these quads. Disregarding an imperfect RM field quality, the target beamlet size is unaffected by the operation of the RMs, and all quadrupoles can be adjusted with a low-power beam mode without operating the RMs. By also minimizing the beamlet size at the CO, this becomes a suitable location for a shield that could limit the intensity of back-streaming neutrons during operation. In Fig. 2, a  $\text{Ø}40$  mm  $\times$  2000 mm aperture is shown centered around the CO beam waist.

In Table 2 the resulting RM parameters are shown. Although the maximum angular centroid ( $\langle w' \rangle_{\max}$ ) is small, it is much larger than the corresponding rms width.

Using TraceWin [6] including 3D space charge, the line's transport of  $5 \times 10^6$  multi-particles has been compared with the linear optics shown in Fig. 2. Contrary to the non-linear magnet layout, the linear model describes the multi-particle simulation well, even to the relative level

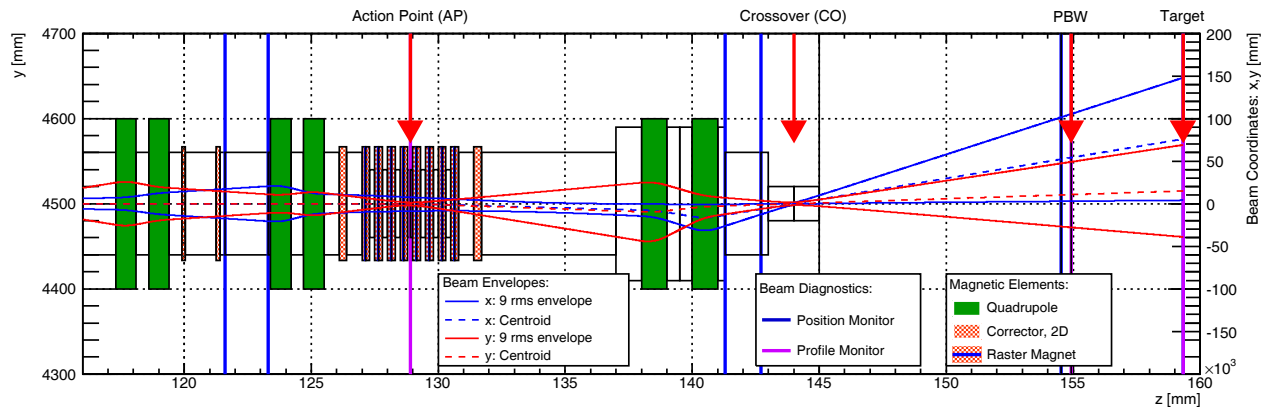


Figure 2: The nominal beam optics at maximum deflection using the parameters of Table 1. The element apertures are indicated by black-lined boxes. At  $E = 2.5$  GeV, the maximum pole tip fields are 0.43 T and 0.62 T in the matching and CO quadrupoles, respectively. The right axis shows the transverse beam coordinates relative to the target centre.

Table 2: RM Parameters and their Impact on the Beam before the CO Doublet

Parameter	Unit	$w = x$	$w = y$
$n_{\text{RM}}$	—	4	4
$(\int BdL)_{\text{max}} / \text{RM}$	mT.m	2.26	2.87
$\langle w' \rangle_{\text{max}}$	mrad	0.818	1.04
$\langle w' \rangle_{\text{max}} / \text{rms}(w')$	—	6.8	2.5

of  $10^{-6}$ , and the beam is transported through the line and CO aperture without any losses. Apparent compliance with a linear model could signify simple operation of the future line.

### Impact of Element Failure

As common-mode failures may not be fully excludable in the RM system design, the beamlet should maintain a minimum size allowing the PBW and target to endure an unrastered beamlet for a considerable duration,  $\approx \Delta t_p$ . The performance of the RMs and their power supplies (PSs) are expected to be monitored by *e.g.*  $\vec{B}$  pickup coils and failure should trigger the machine protection system. Assuming individual powering of the RMs, the impact of a PS failure is greatly reduced. With  $n_{\text{RM}} = 4 + 4$ , full failure of a single RM would reduce the pattern amplitude to 75%, and  $\langle J \rangle$  would increase by up to 33%, depending on  $\text{rms}(w)/a_w$ . Failure of a vertical RM would thus have less effect on  $\langle J \rangle$ . Intensity increases of this magnitude are expected to be tolerable even for a few beam pulses.

Failure of the CO quadrupoles would not only change the beamlet size and pattern amplitude on the target but also violate the CO conditions, possibly leading to beam losses at the CO aperture. Designing these quadrupoles with a large inductance could intrinsically guarantee that the field reduction possible within  $\approx \Delta t_p$  would be modest. Assuming even a 5% reduction (corresponding to about 50 ms of field decay) in either of the CO quadrupoles does not bring

10-rms envelopes in contact with the aperture, but affects the target beamlet parameters.

## CONCLUSION

The principle and optics of a 2D RM beam expander system has been presented. Relying exclusively on linear optics, this system has many advantages. Contrary to the method employing non-linear magnets, the transverse emittance distribution is generally conserved and the transverse halo is not excessively focused when matching the beam to the NFP. Even to high statistics, all multi-particles successfully reach the target. The RM system thus provides a low target and PBW peak current density by virtue of the raster concept, while having a reduced sensitivity towards the linac beam quality of limited predictability. Initial assessment of the RM parameters and the impact of imperfect magnetic field waveforms appear promising, despite the required  $f_y \approx 40$  kHz. The transport line's sensitivity to static element errors are yet to be studied but are expected to be tolerable as only linear elements are involved.

## ACKNOWLEDGEMENTS

To pursue the concept of a raster-based beam expander system was proposed by a group of people at the ESS, who have subsequently also actively participated in other parts of the feasibility study. In particular, we would like to thank Tom Shea, Eric Pitcher, Dave McGinnis, and Carlos Martins for their contributions.

## REFERENCES

- [1] A.I.S. Holm *et al.*, IPAC'12, MOPPD049, p. 475 (2012).
- [2] S. Chapelle *et al.*, LINAC'98, TU4089, p. 612 (1998).
- [3] H. Saugnac *et al.*, IPAC'11, WEPS92, p. 2721 (2011).
- [4] D. Reggiani, HB2012, WEO3A03 (2012).
- [5] B. Blind *et al.*, LINAC 2006, MOP055, p. 171 (2006).
- [6] R. Duperrier *et al.*, ICCS'02, LNCS2331, p. 411 (2002).